iScience

CellPress
OPEN ACCESS

Article

Multistage feedback-driven compartmental dynamics of hematopoiesis

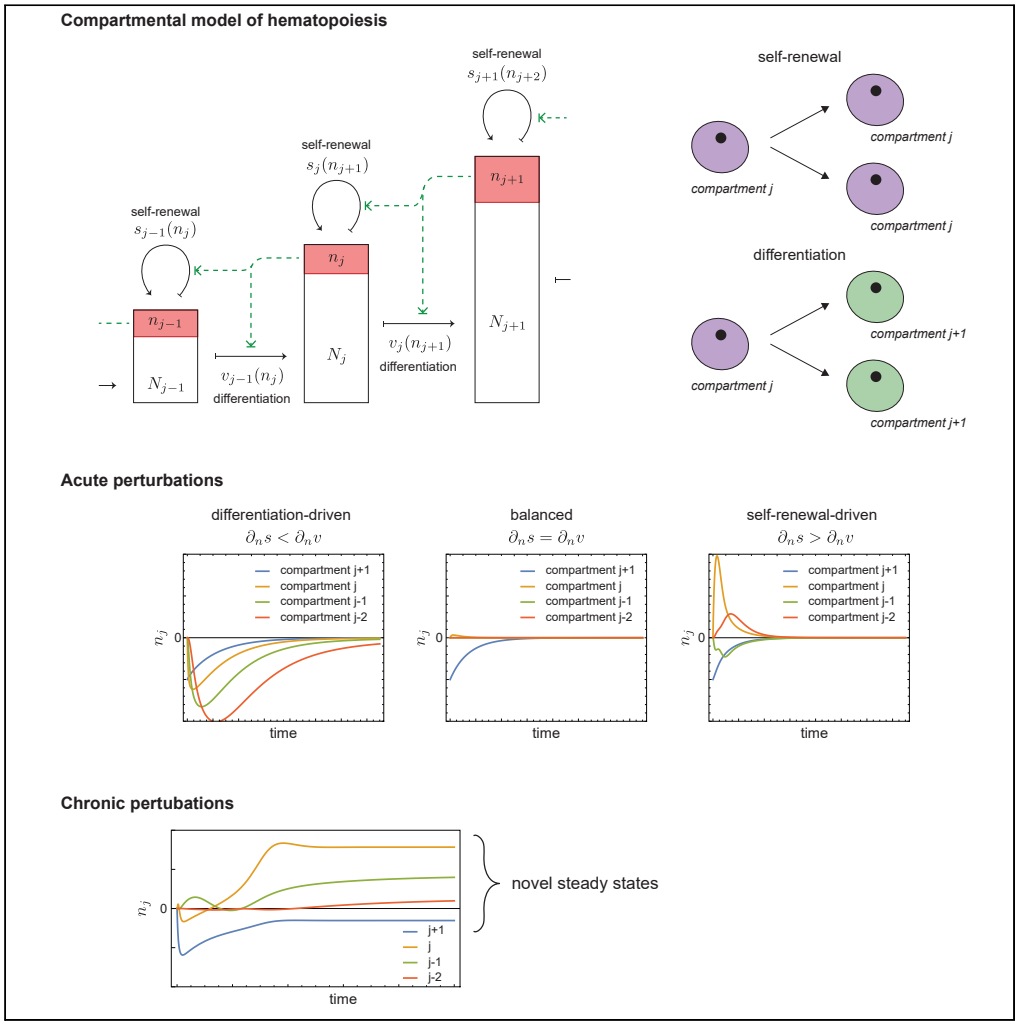

Nathaniel Vincent Mon Père, Tom Lenaerts, Jorge Manuel dos Santos Pacheco, David Dingli

dingli.david@mayo.edu

Highlights

Feedback-driven responses facilitate swift recovery from sudden perturbations

Stability requires balanced adaptation of self-renewal and differentiation

Chronic perturbations result in long-term alterations of the steady state

Mon Père et al., iScience 24, 102326
April 23, 2021 © 2021 The Author(s).
https://doi.org/10.1016/j.isci.2021.102326

iScience

CellPress
OPEN ACCESS

Article

Multistage feedback-driven compartmental dynamics of hematopoiesis

Nathaniel Vincent Mon Père,[1,2,3] Tom Lenaerts,[1,3,4] Jorge Manuel dos Santos Pacheco,[5,6,7] and David Dingli[8,9,*]

SUMMARY

Human hematopoiesis is surprisingly resilient to disruptions, providing suitable responses to severe bleeding, long-lasting immune activation, and even bone marrow transplants. Still, many blood disorders exist which push the system past its natural plasticity, resulting in abnormalities in the circulating blood. While proper treatment of such diseases can benefit from understanding the underlying cell dynamics, these are non-trivial to predict due to the hematopoietic system's hierarchical nature and complex feedback networks. To characterize the dynamics following different types of perturbations, we investigate a model representing hematopoiesis as a sequence of compartments covering all maturation stages—from stem to mature cells—where feedback regulates cell production to ongoing necessities. We find that a stable response to perturbations requires the simultaneous adaptation of cell differentiation and self-renewal rates, and show that under conditions of continuous disruption—as found in chronic hemolytic states—compartment cell numbers evolve to novel stable states.

INTRODUCTION

Hematopoiesis is the physiological process responsible for the production of all circulating blood cells. This includes the oxygen-carrying erythrocytes and several types of white blood cells associated with the innate and adaptive immune response and platelets. The general mechanism follows a hierarchical architecture, with rare slowly replicating multipotent hematopoietic stem cells (HSCs) seeding more differentiated progenitors that increase in frequency through successive levels of maturation (Doulatov et al., 2012; Laurenti and Göttgens, 2018; Notta et al., 2016). Considering the ubiquitous nature of hematopoietic cell types in the body, it is no surprise that we observe many disorders—often hereditary in origin—related to improper development or problematic behavior in the bone marrow (Kaushansky, 2016).

Detailed experimental studies of various aspects of this process can be found dating back to the previous decennium—spanning topics such as HSCs (Eaves, 2015), lineage development (Höfer and Rodewald, 2018; Notta et al., 2016), and signaling pathways (Robb, 2007)—resulting in a qualitatively detailed picture of this architecture. However, from a quantitative viewpoint our collective knowledge is still lacking, in no small part due to the fact that *in vivo* studies of the bone marrow cell dynamics present numerous challenges. Still, in the past decades a handful of mathematical models aimed at understanding the dynamics of hematopoiesis have been developed (Bélair et al., 1995; Bernard et al., 2003; Adimy et al., 2005; Dingli et al., 2007, 2008, 2009; Marciniak-Czochra et al., 2008; Lo et al., 2009; Doumic et al., 2011; Pacheco et al., 2008; Lenaerts et al., 2010; Mon Père et al., 2018; Roeder and Loeffler, 2002; Schirm et al., 2013, 2014, 2018; Krinner et al., 2013; Scholz et al., 2010; Engel et al., 2004; Kirouac et al., 2009, 2010), covering topics such as stem cell organization (Kirouac et al., 2009; Marciniak-Czochra et al., 2008; Mon Père et al., 2018; Roeder and Loeffler, 2002), maturation pathways (Bélair et al., 1995; Doumic et al., 2011; Engel et al., 2004; Krinner et al., 2013; Lo et al., 2009; Schirm et al, 2013, 2014; Scholz et al., 2010), regulatory networks (Kirouac et al, 2009, 2010), and behaviors in selected disease contexts (Adimy et al., 2005; Bernard et al., 2003; Dingli et al., 2009; Lenaerts et al., 2010; Mon Père et al., 2018; Pacheco et al., 2008; Schirm et al., 2018; Werner et al., 2011). Given the complex multicompartment structure of hematopoiesis and its reliance on the presence of cytokines, chemokines, hormones, and the local microenvironment, regulatory feedback loops linking such compartments are expected to be present. These feedback loops likely have important consequences on the overall cell dynamics, especially after the occurrence of perturbations which disrupt normal homeostasis. A number of important models describing selected feedback-driven organizations within the hematopoietic system have been proposed by Loeffler, Scholtz, and colleagues

[1]Interuniversity Institute of Bioinformatics in Brussels, Université libre de Bruxelles – Vrije Universiteit Brussel, 1050 Brussels, Belgium

[2]Applied Physics group, Department of Physics, Vrije Universiteit Brussel, 1050 Brussels, Belgium

[3]Machine Learning Group, Département d'Informatique, Université libre de Bruxelles, 1050 Brussels, Belgium

[4]AI lab, Computer Science Department, Vrije Universiteit Brussel, 1050 Brussels, Belgium

[5]Centro de Biologia Molecular e Ambiental, Universidade do Minho, 4710–057 Braga, Portugal

[6]Departamento de Matemática e Aplicações, Universidade do Minho, 4710–057 Braga, Portugal

[7]ATP-group, P-2744-016 Porto Salvo, Portugal

[8]Division of Hematology and Department of Molecular Medicine, Mayo Clinic, Rochester, MN 55905, USA

[9]Lead contact

*Correspondence: dingli.david@mayo.edu

https://doi.org/10.1016/j.isci.2021.102326

This is an open access article under the CC BY-NC-ND license (http://creativecommons.org/licenses/by-nc-nd/4.0/).

(Engel et al., 2004; Krinner et al., 2013; Schirm et al, 2013, 2014; Scholz et al., 2010), which study compartment-based differentiation dynamics under various pressures such as chemotherapy and growth factor administration. These efforts have demonstrated how such models can provide important insights into the behavior and architecture of the hematopoietic system, as well as aid in predicting the course of treatment strategies against diseased states. As such, understanding the types of dynamical behaviors which may occur under compartmental feedback can be important for understanding the progression of hematopoietic diseases which affect blood cell production, concentration, and development. Here we take a general approach to investigating some properties of this class of systems, with a focus on how perturbations to cell numbers can influence the self-renewal and differentiation behavior of the maturing cells. To this end, we develop a theoretical model which, starting from the description of hematopoiesis developed by Dingli et al. (Dingli et al., 2007), introduces regulatory feedback mechanisms that allow the system to react to perturbations, for example a loss of cells due to bleeding or hemolysis. In the following context, we introduce a general formalism for modeling feedback in linked hierarchical compartments by specifying the requirements of such a coupling without specific knowledge of the coupling function itself. Subsequently, we apply this feedback structure to examine the dynamics of a multistage feedback-driven compartmental model of hematopoiesis, validated using data from a study on erythrocyte dynamics (Hillman and Henderson, 1969). We study possible dynamic behaviors after a perturbation and identify under which conditions these occur. Finally we assess how the behavior changes under chronic perturbations.

RESULTS

Model development

The model of Dingli et al. (Dingli et al., 2007) constitutes our starting point. It describes the maturation process of hematopoietic cells through a fixed number M of discrete compartments associated with progressive "levels" of differentiation that all cells traverse before leaving the bone marrow. Within each compartment j a cell divides at a predefined rate r_j, where each division is considered symmetric (for simplicity), that is, it gives rise to two identical daughter cells. These are either exact replicas of the parent—with probability $1-\varepsilon_j$—and thus remain in the current compartment j, or have differentiated—with probability ε_j—and thus move to the subsequent compartment $j+1$. Under homeostatic conditions the number of cells in each compartment should remain approximately constant in time, while compartment sizes increase toward maturity at a fixed ratio $N_{j+1}/N_j = \eta$ to accommodate the expansion of a small number of stem cells (N_0, of the order of several hundred for humans) to the daily output of the bone marrow ($N_M \approx 10^{11}$). This exponential increase is mirrored by the division rates: $r_{j+1}/r_j = \rho$, while the differentiation probability is taken the same for all maturing compartments: $\varepsilon_j = \varepsilon$. Only for the very first stem cell compartment $\varepsilon_0 = 0.5$ is required, as there is no flux of cells entering it from other compartments. Values for these parameters can be derived by fixing the initial and final compartment sizes and division rates, and using the equilibrium requirement $\partial_t N_j = 0$ (see supplemental information).

In order to address the coupling between compartments through feedback, we now alter the existing formalism. First, we formally describe both types of division—self-renewal ($j \to j$) and differentiation ($j \to j+1$)—as independent Poisson processes occurring with rates v_j and s_j, respectively. It can be shown that this description is equivalent to the original one through the relations $r_j = s_j + v_j$ and $\varepsilon_j = s_j(s_j + v_j)^{-1}$ (see supplemental information for a detailed derivation). The cell dynamics are given by the following equations for cell numbers in each maturing compartment j:

$$\partial_t N_j = 2s_{j-1}N_{j-1} - (s_j - v_j)N_j \qquad \text{(Equation 1)}$$

We furthermore add an additional compartment for cells that reach maturity after leaving the final bone marrow compartment M, the size of which is taken from a recent estimate of the total number of cells in the peripheral blood (Sender et al., 2016): $N_{PB} \approx 10^{13}$. In this compartment cells no longer differentiate; however their number can still decrease due to cell death or destruction. Thus, the first (HSC) and final (peripheral blood) compartments behave according to

$$\begin{aligned} \partial_t N_{HSC} &= -(s_{HSC} - v_{HSC})N_j \\ \partial_t N_{PB} &= 2s_M N_M - \mu_{PB} N_{PB} \end{aligned} \qquad \text{(Equation 2)}$$

where μ_{PB} is the constant (normal) death rate of cells in the peripheral blood compartment. Under homeostatic conditions the system is stable with $N_j(t) = N_j^*$ and $\partial_t N_j^* = 0$, and the division rates are given by their homeostatic values v_j^* and s_j^*. We introduce feedback through sequential coupling between successive compartments, by allowing these division rates of each compartment to vary depending on the number

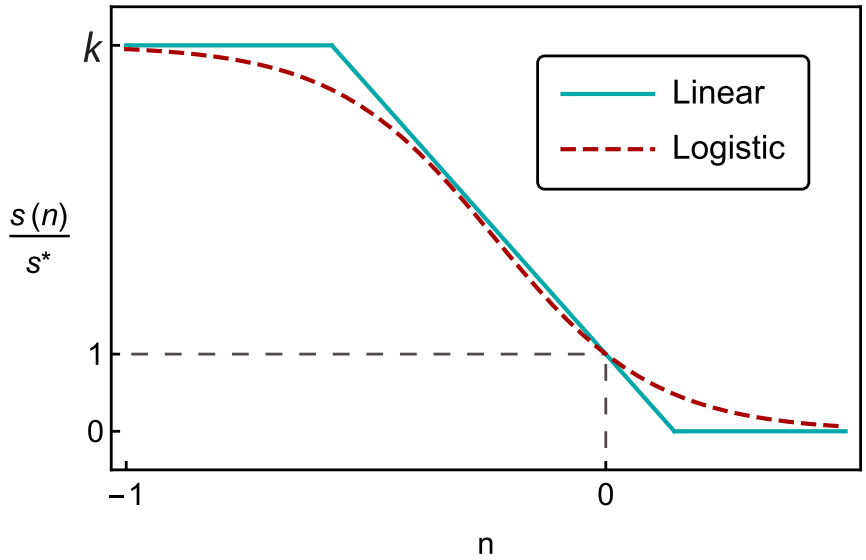

Figure 1. Illustration of linear and logistic differentiation rate functions
Both are bounded between 0 and $k_s s^*$, and have $s(0) = s^*$.

of cells in a neighboring downstream compartment. Given a perturbation $n_i = (N_i - N_i^*)/N_i^*$ on the cell number in compartment i, we are thus looking for non-negative functions $v_j(n_i)$ and $s_j(n_i)$ that produce a negative feedback response—i.e. opposing the sign of n_i. Furthermore, we assume there is an upper limit to how many divisions a cell can undergo in a fixed span of time, thus determining upper bounds on $v_j(n_i)$ and $s_j(n_i)$. Naturally, the fact that homeostasis is maintained in the absence of any perturbation implies that $v_j(0) = v_j^*$ and $s_j(0) = s_j^*$.

From the outset, the functions $v_j(n_i)$ and $s_j(n_i)$are expected to be the solution of a highly non-linear ecological network of various cell types, nutrients, and signaling factors (Otto and Day, 2007). Here, instead, we look for the simplest functional form that fulfills the requirements above; this leads us to the bounded linear form (Figure 1):

$$\theta(n) = \begin{cases} 0, & (1-\alpha_\theta n)<0 \\ \theta^*(1-\alpha_\theta n), & 0>(1-\alpha_\theta n)>k_\theta \\ k_\theta \theta^*, & (1-\alpha_\theta n)>k_\theta \end{cases} \qquad \text{(Equation 3)}$$

where θ represents either v or s. Furthermore, since by conception we are only interested in a coupling which exhibits negative feedback—i.e. where the reaction counteracts the effects of the perturbation—we require $\alpha_\theta \geq 0$. Intuitively, this can be understood as only considering systems in which a *loss* of cells in a compartment causes an *increase* in production in the reacting upstream compartment and an *excess* of cells causes a *decrease* in production, as the converse would result in a positive feedback.

A smoother version is easy to define by drawing inspiration from classical ecological systems, which mirror the competition for promoting or inhibiting factors among different cell groups (Otto and Day, 2007; Strogatz, 2001). In this vein, a logistic function (Figure 1) of the form

$$\frac{\theta(n)}{\theta^*} = \frac{k_\theta}{1+(k_\theta - 1)e^{\alpha_\theta n}} \qquad \text{(Equation 4)}$$

where the parameters k_θ and α_θ play analogous roles in determining respectively the maximum and the slope, constitutes a natural choice.

While the rate functions defined above provide a useful method for coupling any pair of compartments, modeling the full hematopoietic system requires an interaction network that defines the pairwise connections between compartments. Many complex circuits are possible, and the number of potential interaction combinations (through pairs or higher orders) increases dramatically with the number of compartments. Here, we explore a simple case, in which all compartments are coupled sequentially to their downstream

neighbors, so that the rate functions have the form $s_j(n_{j+1})$ and $v_j(n_{j+1})$ for all j. Given this interaction network, as well as the rate functions and their parameters α_s, k_s, α_v, $k_v \in \mathbb{R}^+$, the solution to (1) for M compartments can be obtained numerically through any finite difference method.

Sequential coupling elicits three types of behavior

We start by examining the case in which hematopoiesis proceeds under homeostasis when a perturbation occurs in a single compartment. The response in the absence of feedback mechanisms has been studied previously (Werner et al., 2011) and can be recovered in this model by fixing the division rates to their homeostatic values: $v_j(t) = v_j^*$ and $s_j(t) = s_j^*$. Equation 1 shows that without feedback the compartmental coupling is entirely one-directional and upstream: the dynamics of N_j depends on N_{j-1} but not on N_{j+1}, meaning that compartments will not respond to disturbances taking place in downstream compartments. Still, when a transient perturbation from equilibrium occurs in a given compartment j, the homeostatic equilibrium is eventually restored (Figure 2A), though in the absence of downstream coupling the relaxation time is too long to match real recovery times (Figure 2), as recent studies on blood donations estimate a typical recovery of hemoglobin content within 20–60 days (Kiss et al., 2015; Pottgiesser et al., 2008; Ziegler et al., 2015). In this scenario, while all upstream neighbors $j - k$ remain in homeostatic conditions ($n_{j-k} = 0$) all downstream $j + k$ are affected as the perturbation moves successively through these compartments (Werner et al., 2011).

This behavior will change when feedback—as described above—is introduced: A dependence of N_j on N_{j+1} is now included and a similar wavelike propagation upstream is now expected. In this model we distinguish three types of dynamics which may follow a perturbation, each of which occurs in a particular regime of the feedback parameters α_s, α_v, k_s, and k_v (Supplemental Information S3). These possible responses are illustrated in Figure 2, which shows the system's dynamics following a perturbation in the peripheral blood compartment. In the first regime (Figure 2B) the reacting compartment M (approximately) maintains its homeostatic cell number, $\partial_t n_{j<j+1} = 0$, which effectively prevents the perturbation from propagating upstream. This is achieved by a balanced response of self-renewal and differentiation: the altered rates at which cells are added ($v(n)$) to and removed ($s(n)$) from the compartment result in no net gain (or loss) of cells. While we find that the logistic coupling functions can never perfectly achieve this result, a first-order approximation sets the requirement $\partial_n s(n) = \partial_n v(n)$ (see supplemental information). Introducing the simplification $k_s = k_v \equiv k$, which in the biological sense implies that the maximum division rates which can occur are the same for self-renewal and differentiation, this reduces to

$$\alpha_v = \left(s_j^* \Big/ v_j^*\right)\alpha_s \qquad \text{(Equation 5)}$$

Note that this requirement implies that for a balanced response the slope of $v(n)$ must be steeper than that of $s(n)$ (Figure 2B), since $s_j^* > v_j^*$ (see supplemental information and [11]). Intuitively, this means that as the differentiation rate changes, the self-renewal rate must change even more if the reacting compartment's cell number is to remain unperturbed. In the second regime (Figure 2C), the reacting compartment's cell number is perturbed in the same direction as the original perturbation—becoming reduced if the perturbation is negative (loss of cells) or increased if the perturbation is positive (excess cells)—causing the perturbation to propagate upstream with the same sign as the initial disruption. This occurs when $\partial_n s < \partial_n v$ (in a first order approximation; see supplemental information), which implies the differentiation rate is changing more than the self-renewal rate. We therefore describe this response as being *differentiation-driven*. In the third regime (Figure 2D), the reacting compartment's cell number changes in opposition to the initial perturbation direction, which leads to damped oscillations in the perturbed and upstream compartments. This occurs when $\partial_n v < \partial_n s$ (see supplemental information), corresponding to the converse circumstance where the variation in self-renewal rate dominates, which we denote as the *self-renewal-driven* response. Compared to the non-feedback case (Figure 2A), each of these behaviors reduces the time required for the perturbed compartment to return to equilibrium.

Increasing cell amplification between compartments reduces stability

The number of interacting compartments M also influences the overall dynamics. Note that M need not necessarily be the same as the number of differentiation stages found through traditional methods such as surface marker identification or transcriptional profiling, as our treatment is flexible enough to loosely describe stages of development which interact through feedback, and thus these compartments may encompass multiple maturation stages found in other models. To ensure a meaningful comparison, we change M assuming the same number of cells at the root of the hematopoietic tree and under circulation.

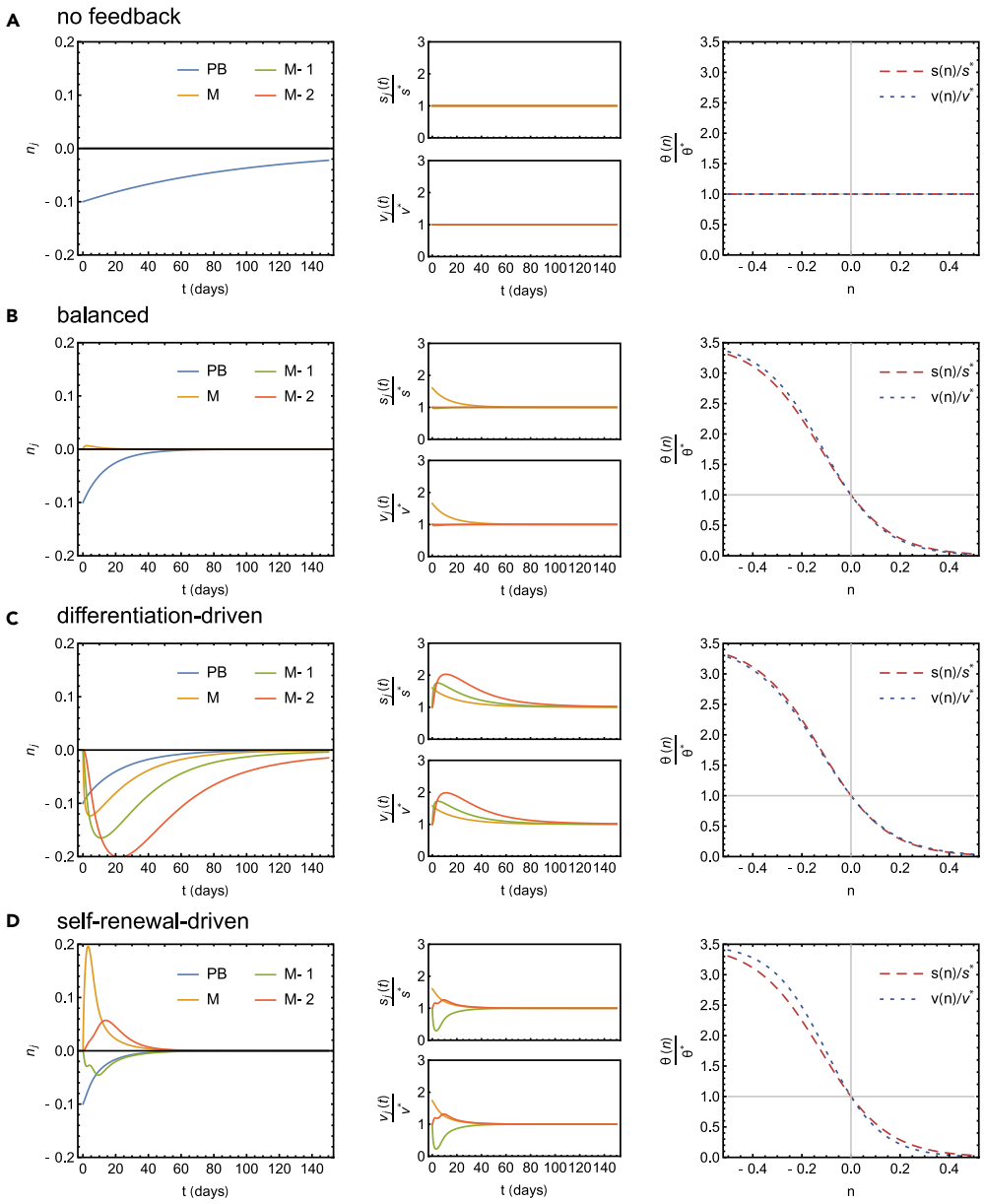

Figure 2. Dynamical behaviors following a perturbation in the peripheral blood compartment for different regimes of the coupling parameters

For each regime (A–D) the dynamics following a perturbation in the peripheral blood compartment is shown for a system with M = 8, and parameters k_s, k_v, and α_s obtained from parameterization to Hillman et al. (Hillman and Henderson, 1969) (see section inclusion of feedback allows prediction of erythrocyte dynamics for details). The first row shows the perturbation n_j on the cell number for the final four compartments (peripheral blood [PB], M, M-1, and M-2) over time. The second row shows the altered differentiation and self-renewal rates as a factor of normal in time. The third row shows the shape of the coupling functions $s(n)$ and $v(n)$. The feedback-free system is shown in (A) and can be obtained by setting α_s and α_v to 0. (B) shows the balanced (to first-order) response where (4) is satisfied. (C) shows the differentiation-driven response with $\alpha_v < (s_j^*/v_j^*)\,\alpha_s$, and (D) shows the self-renewal-driven response where $\alpha_v > (s_j^*/v_j^*)\,\alpha_s$.

Thus, smaller M implies larger cell amplification rates between consecutive compartments. Varying M is found to influence the stability of the hematopoietic system with respect to the rate parameters: when deviations from the balanced response take place, one obtains an increase in amplitude of upstream perturbations with decreasing M (see supplemental information). In this sense, hematopoietic models with lower M are less stable under perturbations on the parameters α_s and α_v. It is worth noting here that stability

under variation of these parameters forms an important requirement for the system itself and will be discussed in detail later.

Recovery time as a measure of efficiency

The time for a compartment to recover from a perturbation is an important measure of the efficiency of hematopoiesis, as an expedited recovery can be considered more advantageous for the host. This recovery time is directly determined by the strength of the response to a loss of cells, which the model itself sets little restriction on: The k and α parameters—respectively determining the maximal increase in divisions and the severity of the perturbation at which this maximal value is reached—can technically (i.e. as long as Equation 5 is fulfilled) be taken arbitrarily high without inducing oscillations or positive feedback. However, in real hematopoiesis one would expect physical limitations to apply to these, such as for example the time and/or resources required for cells to undergo additional divisions. In addressing the recovery time, we should take all possible recovery types into consideration. Indeed, we should keep in mind that hematopoietic cell numbers fluctuate in time even under homeostatic conditions (Kaushansky, 2016). Consequently, it is reasonable to assign some range around the model's equilibrium value within which a compartment can be considered "recovered". For example, while Figure 2B shows a greatly improved response compared to the feedback-free model in 2a, the oscillatory behavior in Figure 2D presents a qualitatively superior result with respect to the recovery time, if we consider a compartment to be recovered once it has returned to within approximately 2% of its homeostatic value. Thus a slight emphasis on self-renewal rather than differentiation in the response can be beneficial if the resulting oscillations are small in amplitude. Conversely, while the regime depicted in 2c (emphasis on differentiation) also improves upon the feedback-free model, it is less efficient than that of 2b, as the resulting positive feedback always reduces efficiency.

As previously noted, realistic estimates for the recovery time after a loss of erythrocytes can be obtained from studies on hemoglobin recovery after blood donation. This procedure comprises the extraction of around 500mL of whole blood and results in a perturbation of $\approx$10% of the baseline hemoglobin mass. One study by Pottgiesser et al. (Pottgiesser et al., 2008) found recovery to within 2% of the baseline value occurring after 20 to 60 days in a cohort of 29 individuals. This timing was corroborated in a later work by Kiss et al. (Kiss et al., 2015), who furthermore found that individual recoveries depended highly on the body's access to iron—both through supplementary intake as well as available iron stores (ferritin)—with the longest recovery times reaching past 150 days in individuals who presented low ferritin levels before donation and did not supplement iron during recovery. These quantities fit well with the dynamics shown in Figure 2, the parameterization of which is discussed in the next section. We note that interestingly the feedback-free scenario captures the recovery time of slowest responding patients in (Kiss et al., 2015), which emphasizes the physical requirements that play a role in facilitating this feedback.

Inclusion of feedback allows prediction of erythrocyte dynamics

To evaluate the predictive power of the model we use data from Hillman et al. (Hillman and Henderson, 1969), who study the human bone marrow response to a severe loss of erythrocytes. The authors mark the increase in erythrocyte production as a function of the normal output for different levels of depletion of the hematocrit, noting that the efficiency of the response depends strongly on the amount of iron available to the patient. We can translate the hematocrit measurements to perturbations in our model by taking the ratio of the depleted to the normal value; for example, if the patient's normal hematocrit is 50%, a reduction to 40% would equate to a 20% loss, which is a perturbation in the bloodstream compartment (B) of $n_B = -0.2$. A summary of their findings is shown in Figure 3. We estimate our parameter values by assuming a balanced response (5) and taking the previously introduced assumption of equal maximum differentiation and self-renewal rates $k_s = k_v \equiv k$. For this coupling the dynamics of the perturbed peripheral blood compartment can be written as $\partial_t n_{PB} = 2s_M - \mu_{PB}(1 + n_{PB})$; with μ_{PB} the constant loss rate of circulating cells, which is independent of the replication rate function $v_M(n_{PB})$ of the preceding compartment. Thus α_v is fixed by the response requirement and only k and α_s are free. A least-squares fit of the logistic coupling (4) results in parameter pairs for the three patient cohorts defined by the authors (based on the patients' body iron stores). The values for the normal patient cohort ($k = 3.5$, $\alpha_s = 7.5$) are used in Figure 2. Different parameter pairs are found for the other cohorts, with a clear effect being an increase in maximal production factor κ for increasing iron availability. This implies that the response relies not only on the severity of the perturbation but on the availability of essential resources as well, so that the parameters α_s, α_v, k_s and k_v should in fact depend on other parameters reflecting a dynamic environment. The values

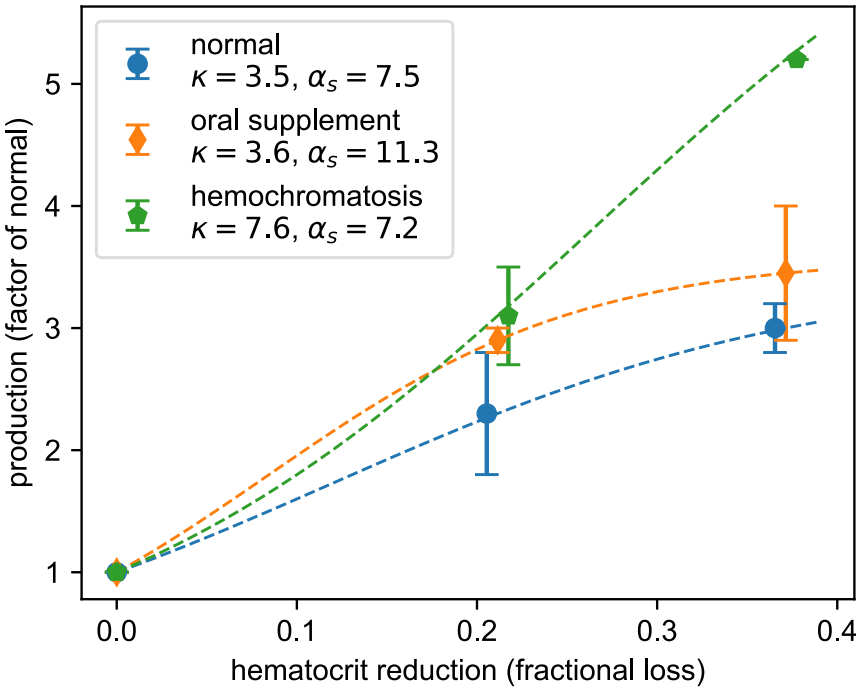

Figure 3. Parameter estimates based on Hillman et al.

Three patient cohorts are defined by the authors (Hillman and Henderson, 1969) based on the size of their available iron stores: a "normal" control group, a group which was administered supplementary iron intakes, and a number of individuals suffering from hemochromatosis, a disorder characterized by an increased amount of total body iron stores. Each production factor shown (symbols) is the center of the range (error bars) measured within a patient cohort, as no individual measurements or averages are specified. Dashed lines result from a least-squares fit to the data employing the logistic coupling model (4), with the assumption that $k_s = k_v = k$, and α_v determined by the balanced response requirement (5).

for $k = k_v = k_s$ found here to range between 3.5 (normal cohort) and 7.6 (hemochromatosis) fit with current knowledge of production rates of mature red blood blood cells, where the highest reported rate increases are 8- to 10-fold the normal rate (Hillman and Henderson, 1969). For this range of k, we thus estimate the slope parameter α_s to be in the range of 7.2–11.3, while α_v is then determined by the compartment number through $\alpha_v = \alpha_s\, s^*/v^*$.

Chronic perturbations lead to new equilibrium states

As a final exploration of the capabilities of the present model, we turn our attention to perturbations with a long-lasting character. These are of particular interest in medicine, as many genetic disorders such as inherited red cell membrane defects (hereditary spherocytosis, elliptocytosis, ovalocytosis), thalassemia syndromes and hemoglobinopathies (sickle cell disease, hemoglobin SC disease) all result in a chronic reduction of red cell survival times and anemia. Autoimmune hemolytic anemia due to autoantibodies against red blood cell antigens can also cause chronic destruction of red blood cells and anemia. We take as a model example the rare but well-studied paroxysmal nocturnal hemoglobinuria (PNH), a life-threatening disease characterized by an acquired mutation in the *PIGA* gene that renders red blood cells susceptible to complement attack resulting in severe hemolysis and other complications (Brodsky, 2014). If the PNH afflicted clone is large enough, a significant portion of circulating erythrocytes will have a severely reduced lifespan. In our model we can take this into account by splitting the peripheral blood compartment into a healthy (*H*) and a PNH afflicted (*PNH*) population, $N_{PB} = N_H + N_{PNH}$, where the death rate of the PNH group is significantly higher than that of the healthy cells ($\mu_{PNH} > \mu_H$). For a clone which comprises a fraction p of bone marrow cells, we obtain the dynamics

$$\begin{cases} \partial_t N_H = 2 s_M(n_{PB})(1-p) N_M(t) - \mu_H N_H(t) \\ \partial_t N_{PNH} = 2 s_M(n_{PB})\, p\, N_M(t) - \mu_{PNH} N_{PNH}(t) \end{cases} \qquad \text{(Equation 6)}$$

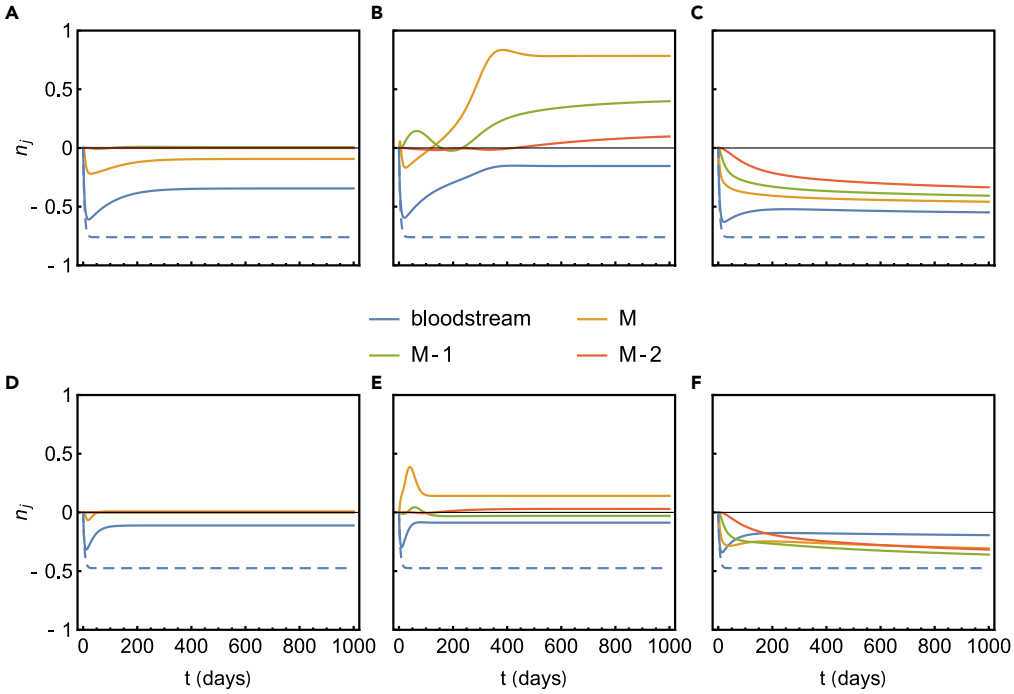

Figure 4. Dynamics following a chronic loss of cells in the bloodstream

(A–F) Responses of an $M = 5$ compartmental model employing logistic coupling with "normal" parameter values taken from Figure 3 (full lines) alongside the feedback-free response (dashed line). The rate of hemolysis of PNH afflicted erythrocytes is taken at $\mu_{PNH} = 0.2$. Two different clone sizes are shown: p = 0.8 (panels (A)–(C)) and p = 0.5 (panels (D)–(F)). Balanced response to clone of size p is shown in panels (A) and (D), self-renewal-driven response ($\partial_n v < \partial_n s$) to clone of size p is shown in panels (B) and (E), and differentiation-driven response ($\partial_n s < \partial_n v$) to clone of size p is shown in panels (C) and (F).

To determine which values of p might occur in humans, we note that PNH clones can comprise up to 100 percent of the blood cell population (Socié et al., 2016), while clones smaller than 10–20% could be considered subclinical. To obtain a realistic value for the rate at which these cells are hemolysed we use a study on the in vivo survival rate of transfused erythrocytes from a PNH afflicted individual (Dacie and Mollison, 1949). While no such death rate is derived in the paper itself, the authors describe a fast initial decay of the transfused population to 50% after only 5 days, followed by a slower decay down to 30% at the 10th day. We can describe this behavior by means of two exponentially decaying populations to estimate the donor's PNH fraction at $p \approx 0.8$ and a death rate of $\mu_{PNH} \approx 0.2$, which means that a PNH erythrocyte will be destroyed after on average 5 days in the bloodstream, 20 times faster than its normal counter-part.

Using the same parameter set derived in the previous section, we observe that, in the long-term, new steady states emerge for all reacting compartments in any response regime (Figure 4). Using Figure 4A as a reference, we observe a marginal improvement in mitigating the loss in the self-renewal-driven regime ($\partial_n v < \partial_n s$) (4b, 4e) whereas, in the differentiation-driven regime ($\partial_n s < \partial_n v$) (4c, 4f) a reduced efficiency is observed. In contrast with the normal recovery that is realized under transient perturbations (Figure 2), the model also predicts a new stationary state for the bloodstream hemoglobin content, which in general remains below the normal homeostatic value. Furthermore, the model captures scenarios where the enduring reduced hemoglobin and red cell mass in circulation is accompanied by a persistent expansion of the upstream compartments (Figures 4B and 4E), as often seen in classic hemolytic PNH as well as other chronic hemolytic disorders (Kaushansky, 2016). As this expansion does not occur in the differentiation-driven regime we conclude that the adaptive response in chronic hemolytic states must (at least) at times take place in a self-renewal-driven regime.

While the dynamics shown in Figure 4 present a reduced displacement of the steady state cell numbers for compartments farther upstream, it is worth noting that this need not be the case in reality. For one, the

parameters of the division rate functions may differ across compartments, allowing for example for higher adaptability in lower numbered compartments. Indeed, one can argue that because cells in the early compartments are slower to act, they can potentially increase their activity to much higher degrees than those in later compartments. Secondly, given the physical necessities such as additional energy and resources required for increasing proliferation, an inability to sustain a drastic response would move that responsibility upstream. This is particularly important for the final compartments, as their higher cell numbers would make such sustained reactions far more costly.

DISCUSSION

The formalism described here provides a simple method for understanding the type of dynamics that populations of maturing hematopoietic cell precursors undergo in the bone marrow after being subject to different types of perturbations (from mild to severe), such as sudden or chronic blood loss. While the starting model of Dingli et al. (Dingli et al., 2007) provides a useful framework for describing the hematopoietic system under homeostatic conditions, it does not account for the dynamics under perturbations such as those discussed here, as the time for a compartment to return to equilibrium is too long to fit clinically observed timescales (Kiss et al., 2015; Pottgiesser et al., 2008; Ziegler et al., 2015). The addition of sequential feedback to the model not only produces swifter recoveries, but also reproduces observed dynamic behaviors such as the response to a transient loss of erythrocytes, and the persistence of anemic states following chronic hemolysis with an associated chronic expansion of precursor cells in the bone marrow. The increased complexity, on the other hand, calls for a careful analysis of the properties of the feedback coupling introduced.

We identify three response types for any coupled pair of compartments, determined by the relative strengths of the differentiation and self-renewal coupling, $s(n)$ and $v(n)$ respectively. A perfectly balanced response prevents the perturbation from moving further upstream, thus providing the simplest reaction profile for hematopoiesis as a whole; it occurs whenever the equality $s(n) - v(n) = s^* - v^*$ is fulfilled, and can intuitively be associated with a response where both differentiation and self-renewal increase (or decrease) in a balanced manner such that the compartment's own cell number remains constant. This is however a very strict condition which is difficult to meet, even on average, in hematopoiesis, given its stochastic nature. Thus one expects that, in general, this detailed balance does not occur, and the dynamic behavior depends on which of the rates comes to dominate. When the differentiation rate dominates, the cell number in the compartment will change in the same direction as the perturbation—decreasing if the perturbation is a loss of cells, increasing if it is an excess—effectively introducing a positive feedback. When the self-renewal rate dominates, the compartment's cell number varies in opposition with the perturbation—increasing with a loss, decreasing with an excess—which can lead to an overcompensation of the loss/excess followed by damped oscillations in the cell number. In some special cases where a resonant condition is met, nearly undamped oscillating cell counts in the blood are observed, associated with extreme cases found in certain hematologic disorders such as cyclic neutropenia (Dingli et al., 2009; Pacheco et al., 2008).

It is important to take into consideration that in real hematopoiesis cell numbers in circulation fluctuate, even under homeostatic conditions (Kaushansky, 2016). Thus it is appropriate to introduce a range of values for the cell numbers within which hematopoiesis can be considered to be in (dynamic) equilibrium. In this sense small oscillations within this range predicted by our model can be presumed to be undetectable (and even if detectable, irrelevant) in a clinical setting. This in turn implies the rate parameters have some leeway to be out of sync without disturbing the bloodstream compartment in a detectable way, adding to the overall robustness of hematopoiesis. This feature, that leads to faster recovery times for small perturbations, may however result in long-lasting perturbations for larger perturbations (Figures 2C and 2D). This highlights the importance of the stability of hematopoiesis with respect to the division rate parameters. Here, the coupling functions $s(n)$ and $v(n)$ posit a deterministic dependency of the division rates on downstream cell counts. In reality, these dependencies will be subject to noise from the underlying stochastic biological circuits and—as already pointed out—are unlikely to have perfectly balanced response solutions in the first place. Furthermore, since the response also depends on the availability of resources (Hillman and Henderson, 1969; Kiss et al., 2015) which may vary or become depleted over time, the balance between s and v adaptation required for stability may itself change in time. However, an important observation is that this stability increases with increasing compartment number, or more specifically decreasing amplification between coupled compartments. The result furthermore adds an interesting angle to the currently favored

view that normal hematopoiesis is mostly driven by "short-term" stem cells which would be found further downstream then the small pool of long-term HSCs (Busch et al., 2015; Sun et al., 2014), as such a larger pool of feedback coupled "drivers" would increase stability.

An important quantifiable characteristic of the feedback-driven system is the strength of the coupling between two compartments (determined by the values of the α and k parameters), as it governs the speed with which a return to equilibrium is attained. We find that while balanced responses (Figure 2B) allow for arbitrarily strong coupling, the physical limit of how fast a single cell can divide of course cannot be exceeded. Furthermore, the coupling strength may also depend on the availability of essential resources, as can be seen from a human erythropoiesis study where individuals with increased access to iron present amplified responses (Hillman and Henderson, 1969), as well as a study of hemoglobin recovery time after blood donation where individuals with more access to iron present a swifter recovery (Kiss et al., 2015). This observation raises the question of how long a particular response can be maintained, especially in the case of persistent losses.

Finally, it is worth remarking upon the differences between the compartmental dynamics under transient and chronic perturbations. In the former case, a short-lived perturbation such as bleeding can be swiftly remedied by increased cell divisions in the higher compartments, without propagating to earlier progenitor stages if the homeostatic balance between self-renewal and differentiation is maintained. In this sense the earliest compartments may not even be requested to respond to an acute loss of blood. On the other hand, chronic perturbations to the system—found in various hematopoietic disorders such as PNH and other hereditary or acquired hemolytic anemias—lead to the emergence of new equilibrium states that do not correspond to normal homeostasis. For example while the altered dynamics might mitigate a persistent loss of erythrocytes due to hemolysis by increasing the bone marrow output, the resulting steady state number of erythrocytes in circulation may still be significantly lower than in the unperturbed system—a scenario which fits the observation of anemia occurring in severe cases of PNH as well as other hereditary or acquired hemolytic states. Experimental data from telomere length analysis in both PNH and sickle cell disease show that circulating mononuclear cells have shorter telomeres compared to age matched controls. Given that in our model self-renewal in any compartment is coupled to replication, this suggests that within hematopoiesis during chronic hemolysis, progenitor and downstream cells are undergoing more self-renewal and thus more replication events than aged matched cells from healthy individuals, leading to shorter telomeres due to attrition with each replication (Karadimitris et al., 2003; Mekontso Dessap et al., 2017). In a former study (Karadimitris et al., 2003), it was found that the shorter telomere length occurred in both PNH afflicted and unafflicted cells, suggesting that the cause indeed lies within hematopoiesis itself, suggesting that the feedback process intrinsic to hematopoiesis does not discriminate between the *PIGA* mutant and normal cells that co-exist in the bone marrow of patients with PNH.

Limitations of the study

The model presented in this work provides insight into the dynamics of a hierarchically structured hematopoietic system; however it should not be considered a diagnostic tool for high accuracy predictions of hematopoietic cell dynamics. The macroscopic approach of combining various regulatory circuits into simple logistic feedback functions—while excellent for interpretive purposes—implicitly neglects potential ongoing processes which could lead to behaviors not captured by the model. For instance, in our model altered division rates depend solely on the perturbed cell numbers, neglecting other influences, such as the availability of resources required for cell division. A possible extension may thus be the inclusion of a dynamic resource pool coupled to hematopoiesis. Another limitation comes from the difficulty of estimating parameter values for the various bone marrow compartments. While fixing the strength of feedback coupling across all compartments is useful for identifying behavioral regimes, there is no available justification for this to be the case in reality. Estimating their different values would require data from *in vivo* measurements of bone marrow cell dynamics, which remains a challenge.

Resource availability

Lead contact

Further information and requests for resources and reagents should be directed to and will be fulfilled by the lead contact, David Dingli (dingli.david@mayo.edu.)

Data and code availability

No data was generated for the work presented in this article. The Mathematica code written for analyzing the model has been made publicly available at https://github.com/natevmp/feedback-driven-hematopoiesis.

METHODS

All methods can be found in the accompanying transparent methods supplemental file.

SUPPLEMENTAL INFORMATION

Supplemental information can be found online at https://doi.org/10.1016/j.isci.2021.102326.

ACKNOWLEDGMENTS

Nathaniel V. Mon Père gratefully acknowledges the funding of Télévie grant nr. 7652018F for supporting the research performed in this work. T.L. acknowledges the support of the F.W.O., through the project nr. G.0259.15, the F.N.R.S., through the project nr. 31257234 and FLAG-ERA JCT 2016 through the Futur-ICT2.0 (www.futurict2.eu) project. Jorge M. Pacheco gratefully acknowledges funding from Fundação para a Ciência e a Tecnologia Portugal through grants PTDC/MAT/STA/3358/2014 and PTDC/MAT-APL/6804/2020.

AUTHOR CONTRIBUTIONS

Conceptualization, N.V.M., T.L., J.M.P., and D.D.; methodology, N.V.M. and J.M.P.; software, N.V.M.; formal analysis, N.V.M. and J.M.P.; writing – original draft, N.V.M., T.L., J.M.P., and D.D.; writing – review & editing, N.V.M., T.L., J.M.P., and D.D.

DECLARATIONS OF INTERESTS

The authors declare no competing interests.

Received: October 13, 2020
Revised: February 2, 2021
Accepted: March 15, 2021
Published: April 23, 2021

REFERENCES

Adimy, M., Crauste, F., and Ruan, S. (2005). A mathematical study of the hematopoiesis process with applications to chronic myelogenous leukemia. SIAM J. Appl. Math. *65*, 1328–1352, https://doi.org/10.1137/040604698.

Bélair, J., Mackey, M.C., and Mahaffy, J.M. (1995). Age-structured and two-delay models for erythropoiesis. Math. Biosci. *128*, 317–346, https://doi.org/10.1016/0025-5564(94)00078-E.

Bernard, S., Bélair, J., and Mackey, M.C. (2003). Oscillations in cyclical neutropenia: new evidence based on mathematical modeling. J. Theor. Biol. *223*, 283–298, https://doi.org/10.1016/S0022-5193(03)00090-0.

Brodsky, R.A. (2014). Paroxysmal nocturnal hemoglobinuria. Blood *124*, 2804–2811, https://doi.org/10.1182/blood-2014-02-522128.

Busch, K., Klapproth, K., Barile, M., Flossdorf, M., Holland-Letz, T., Schlenner, S.M., Reth, M., Höfer, T., and Rodewald, H.-R. (2015). Fundamental properties of unperturbed haematopoiesis from stem cells *in vivo*. Nature *518*, 542–546, https://doi.org/10.1038/nature14242.

Dacie, J.V., and Mollison, P.L. (1949). Survival of transfused erythrocytes from a donor with nocturnal hæmoglobinuria. Lancet *1*, 390–392, https://doi.org/10.1016/S0140-6736(49)90704-7.

Dingli, D., Antal, T., Traulsen, A., and Pacheco, J.M. (2009). Progenitor cell self-renewal and cyclic neutropenia. Cell Prolif. *42*, 330–338, https://doi.org/10.1111/j.1365-2184.2009.00598.x.

Dingli, D., Traulsen, A., and Pacheco, J.M. (2008). Dynamics of haemopoiesis across mammals. Proc. R. Soc. Lond. B: Biol. Sci. *275*, 2389–2392, https://doi.org/10.1098/rspb.2008.0506.

Dingli, D., Traulsen, A., and Pacheco, J.M. (2007). Compartmental architecture and dynamics of hematopoiesis. PLoS One *2*, e345, https://doi.org/10.1371/journal.pone.0000345.

Doulatov, S., Notta, F., Laurenti, E., and Dick, J.E. (2012). Hematopoiesis: a human perspective. Cell Stem Cell *10*, 120–136, https://doi.org/10.1016/j.stem.2012.01.006.

Doumic, M., Marciniak-Czochra, A., Perthame, B., and Zubelli, J. (2011). A structured population model of cell differentiation. SIAM J. Appl. Math. *71*, 1918–1940, https://doi.org/10.1137/100816584.

Eaves, C.J. (2015). Hematopoietic stem cells: concepts, definitions, and the new reality. Blood *125*, 2605–2613, https://doi.org/10.1182/blood-2014-12-570200.

Engel, C., Scholz, M., and Loeffler, M. (2004). A computational model of human granulopoiesis to simulate the hematotoxic effects of multicycle polychemotherapy. Blood *104*, 2323–2331, https://doi.org/10.1182/blood-2004-01-0306.

Hillman, R.S., and Henderson, P.A. (1969). Control of marrow production by the level of iron supply. J. Clin. Invest. *48*, 454–460, https://doi.org/10.1172/JCI106002.

Höfer, T., and Rodewald, H.-R. (2018). Differentiation-based model of hematopoietic stem cell functions and lineage pathways. Blood *132*, 1106–1113, https://doi.org/10.1182/blood-2018-03-791517.

Karadimitris, A., Araten, D.J., Luzzatto, L., and Notaro, R. (2003). Severe telomere shortening in patients with paroxysmal nocturnal hemoglobinuria affects both GPI– and GPI+ hematopoiesis. Blood *102*, 514–516, https://doi.org/10.1182/blood-2003-01-0128.

K. Kaushansky, ed. (2016). Williams Hematology, Ninth edition (McGraw-Hill).

Kirouac, D.C., Ito, C., Csaszar, E., Roch, A., Yu, M., Sykes, E.A., Bader, G.D., and Zandstra, P.W. (2010). Dynamic interaction networks in a hierarchically organized tissue. Mol. Syst. Biol. *6*, 417, https://doi.org/10.1038/msb.2010.71.

Kirouac, D.C., Madlambayan, G.J., Yu, M., Sykes, E.A., Ito, C., and Zandstra, P.W. (2009). Cell–cell interaction networks regulate blood stem and progenitor cell fate. Mol. Syst. Biol. *5*, 293, https://doi.org/10.1038/msb.2009.49.

Kiss, J.E., Brambilla, D., Glynn, S.A., Mast, A.E., Spencer, B.R., Stone, M., Kleinman, S.H., and Cable, R.G.; For the National Heart, L., and Blood Institute (NHLBI) Recipient Epidemiology and Donor Evaluation Study–III (REDS-III) (2015). Oral iron supplementation after blood donation: a randomized clinical trial. JAMA *313*, 575–583, https://doi.org/10.1001/jama.2015.119.

Krinner, A., Roeder, I., Loeffler, M., and Scholz, M. (2013). Merging concepts - coupling an agent-based model of hematopoietic stem cells with an ODE model of granulopoiesis. BMC Syst. Biol. *7*, 117, https://doi.org/10.1186/1752-0509-7-117.

Laurenti, E., and Göttgens, B. (2018). From haematopoietic stem cells to complex differentiation landscapes. Nature *553*, 418–426, https://doi.org/10.1038/nature25022.

Lenaerts, T., Pacheco, J.M., Traulsen, A., and Dingli, D. (2010). Tyrosine kinase inhibitor therapy can cure chronic myeloid leukemia without hitting leukemic stem cells. Haematologica *95*, 900–907, https://doi.org/10.3324/haematol.2009.015271.

Lo, W.-C., Chou, C.-S., Gokoffski, K.K., Wan, F.Y.-M., Lander, A.D., Calof, A.L., and Nie, Q. (2009). Feedback regulation in multistage cell lineages. Math. Biosci. Eng. *6*, 59–82, https://doi.org/10.3934/mbe.2009.6.59.

Marciniak-Czochra, A., Stiehl, T., Ho, A.D., Jäger, W., and Wagner, W. (2008). Modeling of asymmetric cell division in hematopoietic stem cells—regulation of self-renewal is essential for efficient repopulation. Stem Cells Develop. *18*, 377–386, https://doi.org/10.1089/scd.2008.0143.

Mekontso Dessap, A., Cecchini, J., Chaar, V., Marcos, E., Habibi, A., Bartolucci, P., Ghaleb, B., Galacteros, F., and Adnot, S. (2017). Telomere attrition in sickle cell anemia. Am. J. Hematol. *92*, E112–E114, https://doi.org/10.1002/ajh.24721.

Mon Père, N., Lenaerts, T., Pacheco, J.M., and Dingli, D. (2018). Evolutionary dynamics of paroxysmal nocturnal hemoglobinuria. PLoS Comput. Biol. *14*, e1006133, https://doi.org/10.1371/journal.pcbi.1006133.

Notta, F., Zandi, S., Takayama, N., Dobson, S., Gan, O.I., Wilson, G., Kaufmann, K.B., McLeod, J., Laurenti, E., Dunant, C.F., et al. (2016). Distinct routes of lineage development reshape the human blood hierarchy across ontogeny. Science *351*, aab2116, https://doi.org/10.1126/science.aab2116.

Otto, S.P., and Day, T. (2007). A Biologist's Guide to Mathematical Modeling in Ecology and Evolution (Princeton University Press).

Pacheco, J.M., Traulsen, A., Antal, T., and Dingli, D. (2008). Cyclic neutropenia in mammals. Am. J. Hematol. *83*, 920–921, https://doi.org/10.1002/ajh.21295.

Pottgiesser, T., Specker, W., Umhau, M., Dickhuth, H.-H., Roecker, K., and Schumacher, Y.O. (2008). Recovery of hemoglobin mass after blood donation. Transfusion *48*, 1390–1397, https://doi.org/10.1111/j.1537-2995.2008.01719.x.

Robb, L. (2007). Cytokine receptors and hematopoietic differentiation. Oncogene *26*, 6715–6723, https://doi.org/10.1038/sj.onc.1210756.

Roeder, I., and Loeffler, M. (2002). A novel dynamic model of hematopoietic stem cell organization based on the concept of within-tissue plasticity. Exp. Hematol. *30*, 853–861, https://doi.org/10.1016/S0301-472X(02)00832-9.

Schirm, S., Engel, C., Loeffler, M., and Scholz, M. (2014). A combined model of human erythropoiesis and granulopoiesis under growth factor and chemotherapy treatment. Theor. Biol. Med. Model. *11*, 24, https://doi.org/10.1186/1742-4682-11-24.

Schirm, S., Engel, C., Loeffler, M., and Scholz, M. (2013). A biomathematical model of human erythropoiesis under erythropoietin and chemotherapy administration. PLoS One *8*, e65630, https://doi.org/10.1371/journal.pone.0065630.

Schirm, S., Engel, C., Loibl, S., Loeffler, M., and Scholz, M. (2018). Model-based optimization of G-CSF treatment during cytotoxic chemotherapy. J. Cancer Res. Clin. Oncol. *144*, 343–358, https://doi.org/10.1007/s00432-017-2540-1.

Scholz, M., Gross, A., and Loeffler, M. (2010). A biomathematical model of human thrombopoiesis under chemotherapy. J. Theor. Biol. *264*, 287–300, https://doi.org/10.1016/j.jtbi.2009.12.032.

Sender, R., Fuchs, S., and Milo, R. (2016). Revised estimates for the number of human and bacteria cells in the body. PLoS Biol. *14*, e1002533, https://doi.org/10.1371/journal.pbio.1002533.

Socié, G., Schrezenmeier, H., Muus, P., Lisukov, I., Röth, A., Kulasekararaj, A., Lee, J.W., Araten, D., Hill, A., Brodsky, R., et al. (2016). Changing prognosis in paroxysmal nocturnal haemoglobinuria disease subcategories: an analysis of the International PNH Registry. Intern. Med. J. *46*, 1044–1053, https://doi.org/10.1111/imj.13160.

Strogatz, S.H. (2001). Nonlinear dynamics and chaos: with applications to physics, biology, chemistry, and engineering, 2. print. ed, Studies in Nonlinearity (Perseus Books).

Sun, J., Ramos, A., Chapman, B., Johnnidis, J.B., Le, L., Ho, Y.-J., Klein, A., Hofmann, O., and Camargo, F.D. (2014). Clonal dynamics of native haematopoiesis. Nature *514*, 322–327, https://doi.org/10.1038/nature13824.

Werner, B., Dingli, D., Lenaerts, T., Pacheco, J.M., and Traulsen, A. (2011). Dynamics of mutant cells in hierarchical organized tissues. PLOS Comput. Biol. *7*, e1002290, https://doi.org/10.1371/journal.pcbi.1002290.

Ziegler, A.K., Grand, J., Stangerup, I., Nielsen, H.J., Dela, F., Magnussen, K., and Helge, J.W. (2015). Time course for the recovery of physical performance, blood hemoglobin, and ferritin content after blood donation. Transfusion *55*, 898–905, https://doi.org/10.1111/trf.12926.

iScience, Volume *24*

Supplemental information

Multistage feedback-driven compartmental dynamics of hematopoiesis

Nathaniel Vincent Mon Père, Tom Lenaerts, Jorge Manuel dos Santos Pacheco, and David Dingli

Transparent Methods

S1 Original model and equilibrium values

In the model of Dingli et al. (Dingli et al., 2007) the dynamics of a compartment j are given by

$$\partial_t N_j = 2\epsilon\, r_{j-1} N_{j-1} - (2\epsilon - 1) r_j N_j$$

The first term on the right hand side of the equation is the flux of cells coming in from the nearest upstream compartment $j-1$ (where the factor 2 comes from the fact that two daughter cells are created per division), while the second term is the sum of the fluxes of cells being removed due to differentiation (at rate $\epsilon r_j N_j$) and added due to self-renewal (at rate $(1-\epsilon) r_j N_j$). Given the number of HSCs N_0, the number of (non-HSC) compartments M, and the daily bone marrow output μ_M; the homeostatic values N_j^*, r_j^*, and ϵ^* can be found by simultaneously solving the equilibrium condition $\eta\rho = 2\epsilon/(2\epsilon - 1)$, the geometric growth equations $N_j = N_0 \eta^j$ and $r_j = r_0 \rho^j$, and the bone marrow output rate $2\epsilon\, r_M N_M = \mu_M$ for ϵ, η, and ρ. For example, given a system with $M = 28$, $N_0 = 400$, and $\mu_M = 3.5 \times 10^{11}$; the values $\epsilon = 0.82$, $\eta = 1.97$, and $\rho = 1.31$ are obtained. Finally, recent estimates of the number of cells in the peripheral blood in an average adult human (Sender et al., 2016) can be used to take $N_{PB} \approx 3 \times 10^{13}$, and using (2) with the homeostatic condition $\partial_t N_{PB} = 0$, we obtain $\mu_{PB} = \mu_{PB}/N_{PB} \approx 1/100$.

S2 Competing Poisson processes

Consider the events V and S as respectively self-renewal and differentiation divisions, each with (independent) exponentially distributed waiting times with rates v and s. We have

$$\begin{cases} P\{V_t\} = 1 - e^{-vt} \\ P\{S_t\} = 1 - e^{-st} \end{cases} \qquad \begin{cases} f_{t_V}(\tau) = v e^{-v\tau} \\ f_{t_S}(\tau) = s e^{-s\tau} \end{cases}$$

with $P\{X_t\}$ the probability of at least one event X occurring in time t and $f_{t_X}(\tau)$ the density distribution of the waiting times. We now introduce the event $\widetilde{V_t}$ as the occurrence of at least one V, occurring before any S in t; and the complementary event $\widetilde{S_t}$ with the converse definition. Note that $\widetilde{V_t}$ and $\widetilde{S_t}$ are mutually exclusive, and cover all possible outcomes except for those where no S or V occur in t. In our biological system these can be interpreted as two competing processes within the cell, where the first event to occur determines the divisional fate. We may write them equivalently as the following sets:

$$\begin{cases} \widetilde{V_t} = \{V_t \cap S_t^c\,, V_t \cap S_t \cap (t_v - t_s)\} \\ \widetilde{S_t} = \{S_t \cap V_t^c\,, S_t \cap V_t \cap (t_s - t_v)\} \end{cases}$$

Since both events in each set are mutually exclusive we may write the probabilities of $\widetilde{V_t}$ and $\widetilde{S_t}$ as the sum of the probabilities of their respective elements. The first term is

$$P\{V_t \cap S_t^c\} = P\{V_t\} P\{S_t^c\} = e^{-st}(1 - e^{-vt})$$

since V_t and S_t are independent (with the analogous argument for $P\{S_t \cap V_t^c\}$). For the second term we obtain

$$\begin{aligned} P\{t_v < t_s \cap S_t \cap V_t\} &= P\{t_v < t_s \cap S_t\} \\ &= \int_0^t P\{t_v < \tau\} f_{t_s}(\tau)\, d\tau \\ &= \int_0^t (1 - e^{-v\tau}) s\, e^{-s\tau}\, d\tau \\ &= 1 - e^{-st} + \frac{s e^{-t(s+v)} - s}{s+v} \end{aligned}$$

and summing the two gives

$$P\{\widetilde{V_t}\} = \frac{v}{s+v}\left(1 - e^{-(s+v)t}\right)$$

From this we identify $\left(1 - e^{-(s+v)t}\right) = P\{V_t \cup S_t\}$, which is the probability of any division (self-renewal or differentiation) occurring in t. Thus $P\{\widetilde{V_t}\}$ and $P\{\widetilde{S_t}\}$ can readily be interpreted as the probabilities of a division occurring in t, multiplied by a probability which determines whether that division is a self-renewal or a differentiation. The above expression can furthermore be expanded for an infinitesimal timestep dt to obtain a rate (Feller, 2009):

$$P\{\widetilde{V_{dt}}\} = \frac{v}{s+v}(s + v)dt + \vartheta(dt^2)$$

which makes it clear that differentiation and self-renewal occur at rates s and v respectively, and allows us to identify $\epsilon = s/(s+v)$ and $r = s + v$.

S3 Determining the response regimes following a transient perturbation

To understand the parameter regimes where each of the three observed behaviors occurs, we examine the simplest possible network with just a single coupled "pair", and turn our attention to the state of the system at time t_0 immediately after a perturbation n_{j+1} is introduced, so that n_j is still 0. With $N_j(t) = N_j^*\left[1 + n_j(t)\right]$, the dynamics of the reacting compartment j given by (1) can then be written as

$$\partial_t\left(N_j^*\left[1 + n_j(t)\right]\right)\big|_{t_0} = 2s_{j-1}\left(n_j(t_0)\right)N_{j-1}^*\left[1 + n_{j-1}(t_0)\right] - \left[s_j\left(n_{j+1}(t_0)\right) - v_j\left(n_{j+1}(t_0)\right)\right]$$

and since at t_0 we still have $n_j(t_0) = 0$ and $n_{j-1}(t_0) = 0$, this reduces to

$$\partial_t n_j\big|_{t_0} = \frac{2s_{j-1}^*}{\eta} - \left(s_j(n_{j+1}) - v_j(n_{j+1})\right) \tag{7}$$

where we again used the shorthand $\eta = N_j^*/N_{j-1}^*$ for the cell amplification between homeostatic compartments. We note that the response type is given by the sign of the left hand side: if $\partial_t n_j\big|_{t_0} = 0$ the reacting compartment j does not change in size, if $\text{sign}\left(\left[\partial_t n_j\big|_{t_0}\right]\right) = \text{sign}(n_{j+1})$ then the reacting compartment is perturbed in the same direction as the initial perturbation, and if $\text{sign}\left(\left[\partial_t n_j\big|_{t_0}\right]\right) \neq \text{sign}(n_{j+1})$ then the reacting compartment is perturbed in the opposite direction of the initial perturbation. In the first case the left hand side of (7) being 0 implies the homeostatic case of (1) is obtained, so that the right hand side leads to

$$s_j(n_{j+1}) - v_j(n_{j+1}) = s_j^* - v_j^* \tag{8}$$

In a biological sense, this means that the amounts of differentiations and self-renewals in the reacting compartment change in a mutually balanced manner such that the cell number does not vary. While (7) can be solved for linear coupling functions (2) to obtain

$$\alpha_v = \left(s_j^*/v_j^*\right)\alpha_s \tag{9}$$

there is no solution to (8) in the case of the logistic coupling, meaning such a system could only approximate this equality. To further investigate the regimes in which (8) is not satisfied, we expand the rate functions about $n_{j+1} = 0$, which after cancellation of the zeroth order terms (due to the homeostatic condition) gives:

$$\partial_t n_j\big|_{t_0} = -\left(\frac{\partial s_j}{\partial n_{j+1}}\bigg|_0 - \frac{\partial v_j}{\partial n_{j+1}}\bigg|_0\right)n_{j+1} + \vartheta\left(n_{j+1}^2\right). \tag{10}$$

Recalling that we have required $\partial s_j/\partial n_{j+1} < 0$ and $\partial v_j/\partial n_{j+1} < 0$ to ensure negative feedback, we can determine the behavioral regime up to first order (i.e. ignoring higher order terms $\vartheta\left(n_{j+1}^2\right)$) from the sign of the bracketed expression on the right hand side. We can see that if $\partial_n s = \partial_n v$ then $\partial_t n_j \approx 0$ and we are (approximately) in the balanced response regime (Fig 2b). For logistic coupling functions and the simplification $k_s = k_v \equiv k$, this requirement reduces to (9). For both perturbations n_j and n_{j+1} to have the same sign (Fig 2c) we require $\partial_n s < \partial_n v$, which – since both $s(n)$ and $v(n)$ are decreasing functions – implies that the rate of differentiation changes faster with n than the rate of self-renewal. This puts us in the differentiation-driven regime (see main text). If n_j and n_{j+1} have opposite signs (Fig 2d) then $\partial_n v < \partial_n s$, in which case the self-renewal adaptation is dominant and we are in the self-renewal-driven regime (see main text).

S4 Compartment cell amplification M determines stability of the system

If the response to a perturbation is not balanced (i.e. $\partial_t n_{j<j+1} \neq 0$), the amplitude of the upstream perturbations will depend on the amplification between compartments η and therefore also the total number of coupled compartments M. The origin for this can be seen by employing the linear coupling functions (3) (which is equivalent to keeping only the linear terms in the logistic function) in determining the response type in equation (10): the inequality in the first derivative becomes $\alpha_v/\alpha_s \neq s^*/v^*$, meaning that the strength of the reacting compartment's perturbation (left hand side of (10)) is determined by how much α_v/α_s deviates from s^*/v^*, the ratio of homeostatic division rates. One can see that the smaller this ratio is, the stronger the impact of deviations (i.e. perturbations on α_v and α_s) from it become. Furthermore, it can be shown that s^*/v^* decreases monotonically with increasing cell number amplification η between compartments, which in our model is akin to decreasing M.

Supplemental References

Feller, W., 2009. An introduction to probability theory and its applications. Vol. 1, 3. ed., rev. print., [Nachdr.]. ed, Wiley series in probability and mathematical statistics. Wiley, S.l.

Sender, R., Fuchs, S., Milo, R., 2016. Revised Estimates for the Number of Human and Bacteria Cells in the Body. PLOS Biology 14, e1002533. https://doi.org/10.1371/journal.pbio.1002533